6-1998

Metabolic Bypass of the Tricarboxylic Acid Cycle during Lipid Mobilization in Germinating Oilseeds: Regulation of NAD+-Dependent Isocitrate Dehydrogenase Versus Fumarase

Kimberly L. Falk
University of Idaho

Robert H. Behal
Iowa State University

Chengbin Xiang
Iowa State University

David J. Oliver
Iowa State University, doliver@iastate.edu

Plant Physiol. (1998) 117: 473–481

Metabolic Bypass of the Tricarboxylic Acid Cycle during Lipid Mobilization in Germinating Oilseeds[1]

Regulation of NAD$^+$-Dependent Isocitrate Dehydrogenase Versus Fumarase

Kimberly L. Falk[2], Robert H. Behal, Chengbin Xiang, and David J. Oliver*

Department of Microbiology, Molecular Biology and Biochemistry, University of Idaho, Moscow, Idaho 83844 (K.L.F.); and Department of Botany, Iowa State University, Ames, Iowa 50010 (R.H.B., C.X., D.J.O.)

Biosynthesis of sucrose from triacylglycerol requires the bypass of the CO_2-evolving reactions of the tricarboxylic acid (TCA) cycle. The regulation of the TCA cycle bypass during lipid mobilization was examined. Lipid mobilization in *Brassica napus* was initiated shortly after imbibition of the seed and proceeded until 2 d postimbibition, as measured by in vivo [1-^{14}C]acetate feeding to whole seedlings. The activity of NAD$^+$-isocitrate dehydrogenase (a decarboxylative enzyme) was not detected until 2 d postimbibition. RNA-blot analysis of *B. napus* seedlings demonstrated that the mRNA for NAD$^+$-isocitrate dehydrogenase was present in dry seeds and that its level increased through the 4 d of the experiment. This suggested that NAD$^+$-isocitrate dehydrogenase activity was regulated by posttranscriptional mechanisms during early seedling development but was controlled by mRNA level after the 2nd or 3rd d. The activity of fumarase (a component of the nonbypassed section of the TCA cycle) was low but detectable in *B. napus* seedlings at 12 h postimbibition, coincident with germination, and increased for the next 4 d. RNA-blot analysis suggested that fumarase activity was regulated primarily by the level of its mRNA during germination and early seedling development. It is concluded that posttranscriptional regulation of NAD$^+$-isocitrate dehydrogenase activity is one mechanism of restricting carbon flux through the decarboxylative section of the TCA cycle during lipid mobilization in germinating oilseeds.

Upon germination of oilseeds, storage triacylglycerols are mobilized by conversion to carbohydrates for transport to the root and shoot axes of the developing seedling. Suc, the major carbohydrate transport form, is used as a substrate for biosynthesis and is respired for energy. Lipid mobilization in postgerminative oilseeds requires the metabolic coordination of four subcellular compartments: the oil body, the glyoxysome, the mitochondrion, and the cytosol (Trelease and Doman, 1984). The elucidation of this complex interaction was dependent on the discovery of the glyoxylate cycle (Kornberg and Krebs, 1957). Fatty acids are cleaved by lipases from their glycerol backbone in the oil body and, after being transported to the glyoxysome, are degraded by β-oxidation to acetyl-CoA. The glyoxylate cycle ultimately catalyzes the condensation of two of these acetyl-CoA molecules to form succinate, which is then transported to the mitochondrion and metabolized by a partial TCA cycle. Since the complete TCA cycle catalyzes two decarboxylative reactions, the quantitative conversion of lipid to Suc can occur only if certain TCA cycle reactions are bypassed. During gluconeogenesis, only the TCA cycle activities of succinate dehydrogenase, fumarase, and malate dehydrogenase are required. The activities of the TCA cycle decarboxylative enzymes NAD$^+$-IDH and α-ketoglutarate dehydrogenase are avoided.

Flux through the TCA cycle in plant tissues can vary, depending on the metabolic requirements of the tissue. For example, a reduction in the activity of the TCA cycle in the light compared with its activity in the dark has been documented (Gemel and Randall, 1992; Hanning and Heldt, 1993). The TCA cycle is regulated by the redox state of the pyridine nucleotide pool (Oliver and McIntosh, 1995). NADH competitively inhibits the activities of NAD$^+$-IDH, α-ketoglutarate dehydrogenase, and pyruvate dehydrogenase (although technically not a component of the TCA cycle, the pyruvate dehydrogenase complex is the entry point of glycolytically derived pyruvate into the TCA cycle). Furthermore, NAD$^+$-IDH is noncompetitively inhibited by NADPH (McIntosh and Oliver, 1992). The regulation of the TCA cycle in plants differs from its regulation in animals in that none of the plant enzymes appears to be controlled by ratios of adenine nucleotides, e.g. the ratio of ATP/ADP or of acetyl-CoA/CoA (Voet and Voet, 1990; Oliver and McIntosh, 1995).

The proposed TCA cycle bypass was first demonstrated by in vivo labeling studies in castor bean endosperm (Canvin and Beevers, 1961). Radiolabeled acetate was shown to be converted into carbohydrate with an experimental efficiency of 70% for the methyl carbon of acetate and 30% for the carboxyl carbon of acetate. The efficiency of conversion was lower for the carboxyl carbon because it is this carbon that is lost from succinate at the reaction of PEP carboxykinase, the only decarboxylative step of gluconeogenesis. In

[1] This research was supported by the National Science Foundation (grant IBN-9696154) and is a publication of the Iowa Agriculture Experiment Station.

[2] Present address: Max-Planck-Institute fuer Chemische Oekologie, 07743, Jena, Germany.

* Corresponding author; e-mail doliver@iastate.edu; fax 1–515–294–1337.

Abbreviations: IDH, isocitrate dehydrogenase; TCA, tricarboxylic acid.

later work, germinating castor bean mitochondria were shown to rapidly oxidize succinate and malate plus glutamate, whereas the TCA cycle intermediates in the decarboxylative portion of the TCA cycle (isocitrate through succinate) were only slowly oxidized (Millhouse et al., 1983). A more recent report addressed the regulation of this bypass at the enzymatic level in cucumber (*Cucumis sativus*) seedlings (Hill et al., 1992). In this study several physiological and enzymological measurements of postgerminative cucumber seedlings were conducted and it was concluded that fumarase and NAD^+-IDH activities are regulated differently. Their data are consistent with a reduction in carbon flux through the decarboxylative reactions of the TCA cycle during lipid mobilization in cucumber cotyledons. Furthermore, the authors compared fumarase and NAD^+-IDH activities in both the light and the dark in postgerminative seedlings and determined that, whereas fumarase activity was unaffected, NAD^+-IDH activity was significantly reduced in the dark. These data suggest that new carbon fixation by photosynthesis is required for full TCA cycle activity. Recently, it was suggested that the TCA cycle may be limited postgerminatively by transcriptional control of mitochondrial pyruvate dehydrogenase (Grof et al., 1995).

We are interested in the developmental regulation of mitochondrial function. Understanding the switch in the role of the mitochondrion in lipid mobilization to its oxidative function during photosynthesis will further our knowledge of mitochondrial biogenesis and mitochondrial development. To this end, we have re-examined and extended the observations of earlier workers (Canvin and Beevers, 1961; Millhouse et al., 1983; Hill et al., 1992, 1994) using a biochemical and molecular approach with *Brassica napus,* Arabidopsis, and cucumber. We show that during the period of maximum gluconeogenesis the presence of NAD^+-IDH was not detectable, either catalytically or immunologically, whereas fumarase activity was easily accounted for. We will present evidence that the posttranscriptional regulation of NAD^+-IDH prevents its activity during gluconeogenesis in germinating *B. napus*.

MATERIALS AND METHODS

Plant Material and Chemicals

For germination and early seedling development studies, *Brassica napus* var Humus and cucumber (*Cucumis sativus*) seeds were allowed to imbibe for 8 to 12 h with aeration before being planted in fine vermiculite. For light-grown tissue, plants were placed in a 22°C room under a 16-h light regime. For analysis of mature leaf tissues, *B. napus*, cucumber, pea (*Pisum sativum*), or Arabidopsis seeds were planted on 1 part soilless mixture:1 part vermiculite and placed in a greenhouse where light duration was 16 h/d and temperature was maintained at 22°C. Cauliflower (*Brassica oleracea*) for immunoblot analysis was obtained from a local grocery store. All chemicals were purchased from Sigma unless otherwise noted. [1-^{14}C]acetate was purchased from NEN.

In Vivo Labeling

Each 10-mL flask contained 0.2 g of cotyledons (after seed coats were removed) or whole seedlings in 1 mL of 10 mM Mes, pH 5.2, and 0.5 μmol of sodium [1-^{14}C]acetate (1 Ci/mol). Evolved $^{14}CO_2$ was collected on a paper wick wet with 20 μL of 5 M KOH. After 30 min of incubation at 30°C in the light, the wick was removed and the reaction was stopped by boiling the tissue in 70% ethanol. After cooling on ice, the tissue was homogenized with a Ten-Broeck homogenizer (Thomas Scientific) and applied to a Dowex-1 formate column (pre-equilibrated in 1 M sodium formate and then washed in water) and then to a Dowex-50 column (pre-equilibrated in 0.1 M HCl and washed in water). The nonpolar eluent containing total carbohydrates was subjected to liquid-scintillation counting. To control for the efficiency of carbohydrate extraction, one sample of each time was spiked with 0.1 μCi of [U-^{14}C]Glc (1.2 Ci/mol) after the tissue was cooled.

Lipid Extraction

Tissue was ground in liquid N_2 to a fine powder and extracted with $CHCl_3$:methanol (v/v, 2:1) at a ratio of 0.5 g tissue to 10 mL of solvent. After 2 h of extraction, particulate matter was removed by filtration. The filtrate was back-extracted with 2.5 mL of 1% NaCl and the organic phase was delivered to a tared vial and dried under an N_2 stream at room temperature to a constant weight.

Isolation of Mitochondria

Mitochondria were prepared from *B. napus* developmentally staged seedlings, Arabidopsis mature leaves, etiolated pea seedlings, and green cucumber seedlings by a modification of the method of Hill et al. (1992). Chilled tissue was homogenized in 3 volumes of the following buffer: 0.3 M sorbitol, 10 mM KH_2PO_4, 2 mM EDTA, 2 mM $MgCl_2$, 2 mM Gly, 1% PVP-40, 1% defatted BSA, 30 mM ascorbate, 25 mM sodium PPi, 14 mM β-mercaptoethanol, 1% polyvinylpolypyrrolidone, 1 mM benzamidine, and 0.1 mM PMSF, pH 7.6. This homogenate was filtered and mitochondria were collected by differential centrifugation, washed, and purified on a Percoll gradient. The mitochondria were washed in BSA-free medium, and the final pellet was suspended in a minimal volume of 20 mM Mops and 5 mM β-mercaptoethanol, pH 7.5, and frozen. The mitochondria were subjected to two freeze-thaw cycles and centrifuged at 12,000*g* for 15 min, and the supernatant was collected for enzyme assays, protein assays, and immunoblot analysis.

Enzyme and Protein Assays

NAD^+-IDH activity was assayed as previously described (McIntosh and Oliver, 1992). The isocitrate- and enzyme-dependent reduction of NAD^+ was monitored by the increase in A_{340} of a 1-mL reaction. The reaction consisted of 20 mM Mops (pH 7.5), 5 mM $MgSO_4$, 5 mM β-mercaptoethanol, 1 mM NAD^+, and 10 mM isocitrate. Fumarase activity was assayed by following the increase in

A_{240} of a 1-mL reaction containing 20 mM Mops (pH 7.5) and 10 mM malate (Behal and Oliver, 1997). Protein concentration was determined by the Bio-Rad Bradford protein assay reagent using ovalbumin as a standard.

cDNA Clones Used

Three cDNA clones were used in this study: *idhI* (accession no. U81993, Behal and Oliver, 1998), *idhII* (accession no. U81994, Behal and Oliver, 1998), and *fum* (accession no. U82201, Behal and Oliver, 1997).

Antibody Preparation

To obtain Arabidopsis IDH I protein for antibody preparation, IDH I was overexpressed in *Escherichia coli*. The cDNA for the mature IDH I protein was amplified by PCR using appropriate primers and cloned into the expression vector pET-24c (Novagen, Inc., Madison, WI). The construct was checked by sequencing to confirm that *idhI* had been cloned as a translational fusion with an N-terminal T7-tag. pET-IDH I was transformed into competent BL21(DE3) *E. coli* cells. SDS-PAGE-purified protein from isopropylthio-β-galactoside-induced cells was submitted to HTI Bio-Products, Inc. (Ramona, CA) for antibody production in rabbits. Resulting antiserum was enriched for IDH-specific IgGs by purification on a column matrix of immobilized IDH I following the manufacturer's instructions (AminoLink, Pierce). Purified anti-IDH was used at a dilution of 1:20 for all *B. napus* immunoblots but detected the recombinant protein and the native Arabidopsis protein at a higher dilution (1:2000). Antibodies against fumarase (Behal and Oliver, 1997) and IDH II (Behal and Oliver, 1998) were produced from cDNA clones by similar protocols.

Immunoblot Analysis

SDS-PAGE on 12.5% acrylamide gels was performed as described by Laemmli (1970). Proteins were transferred to a nitrocellulose membrane in modified Towbin buffer (25 mM Tris, 192 mM Gly, and 10% methanol, pH 8.3) (Towbin et al., 1979). Secondary antibody was goat anti-rabbit alkaline phosphatase conjugate using 5-bromo-4-chloro-3-indolyl phosphate and nitroblue tetrazolium as the colorigenic substrates.

RNA Analysis

Total RNA was extracted from developmentally staged *B. napus* and cucumber seedlings as previously described for *Aspergillus nidulans* (Timberlake, 1986) with one modification: dry seed and d 1 and 2 postimbibition RNA was differentially precipitated with 2-butoxyethanol to remove interfering polysaccharides, as described by Schultz et al. (1994). RNA was electrophoresed in formaldehyde gels and blotted to nylon as summarized by Sambrook et al. (1989). Loading was standardized with rRNA. Polysomes were extracted from 1-d-old postimbibition *B. napus* seedlings, according to the method of DeVries et al. (1988), except that 250 μM β-mercaptoethanol was added to the extraction buffer. RNA was extracted from polysomes by phenol-chloroform extraction (Timberlake, 1986).

RESULTS

Time Course of Lipid Mobilization during *B. napus* Seedling Development

The relationship between gluconeogenesis and lipid mobilization in developing *B. napus* seedlings is demonstrated in Figure 1. Carbohydrate synthesis from fatty acids was measured as the ratio of $^{14}CO_2$ released to [^{14}C]carbohydrate synthesized when seedlings were fed [1-^{14}C]acetate (Fig. 1, right *y* axis). When plant tissue is utilizing lipid as a carbon and energy source, the ratio of released $^{14}CO_2$ to synthesized [^{14}C]carbohydrate will be lower than when photosynthate is the sole carbon and energy source (Canvin and Beevers, 1961). Figure 1 shows that the ratio of [1-^{14}C]acetate incorporation into $^{14}CO_2$ to [^{14}C]carbohydrate was 1.08 ± 0.09 for light-grown and 1.48 ± 0.16 for dark-grown *B. napus* seedlings at 12 h postimbibition. The difference between light- and dark-grown seedlings was significant by a Student's *t* test. By comparison, Canvin and Beevers (1961) measured a $^{14}CO_2$ to ^{14}C-carbohydrate ratio of 1:1 in 5-d-old castor bean endosperm when it was labeled with [1-^{14}C]acetate. Although the metabolism of en-

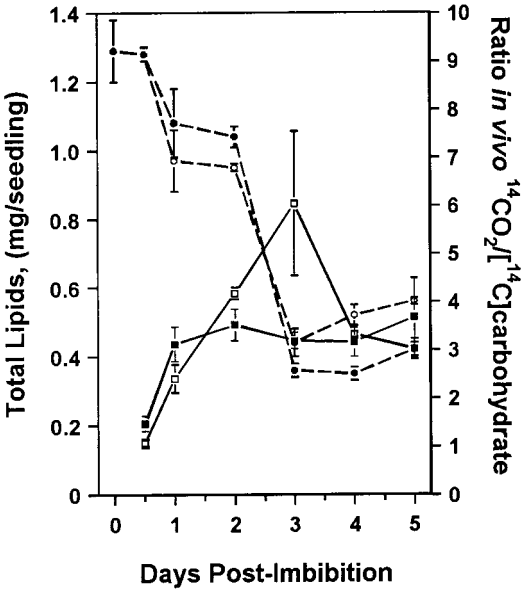

Figure 1. Lipid data on the left *y* axis represent total lipid of seedlings calculated as the means ± SD of three replicate measurements per data point. ○, Lipid content in light-grown seedlings; ●, lipid content in dark-grown seedlings. In vivo labeling data (the ratio of $^{14}CO_2$ released from [1-^{14}C]acetate to ^{14}C incorporated into the neutral fraction containing soluble sugars) on the right *y* axis represent the means ± SD for three replicates per data point. Analysis of in vivo labeling results by a Student's *t* test showed that data for d 0.5 and 3 were significantly different between dark and light at $P < 0.05$. Days 1, 2, 4, and 5 were not significantly different between light and dark at $P < 0.05$. □, Labeling ratio for light-grown seedlings; ■, labeling ratio for dark-grown seedlings.

dospermic seeds and nonendospermic (cotyledonary) seeds cannot be directly compared, our measurement indicates that the fate of [1-^{14}C]acetate is primarily gluconeogenic in *B. napus* seedlings at 12 h postimbibition.

Under the growth conditions in our laboratory, germination occurred at 12 h postimbibition. The ratio of $^{14}CO_2$ to ^{14}C-carbohydrate increased after germination, indicating an increase in CO_2 evolution by the TCA cycle, until 2 d postimbibition, reaching a typical value of about 4:1 for both light- and dark-grown seedlings. At 2 d postimbibition, the ratio of CO_2 evolved to carbohydrate synthesized was relatively constant in both light- and dark-grown seedlings, with the exception of a peak of respiration in the 3-d postimbibition light-grown seedlings. We have no physiological explanation for this unexpectedly high ratio, although it was observed in all three replications of this experiment. At 3 d postimbibition the cotyledons were beginning to turn green and by 4 d postimbibition were fully photosynthetic. Thus, at 12 h postimbibition acetate appeared to be exclusively metabolized to carbohydrates. From 12 h to 2 or 3 d postimbibition acetate was increasingly metabolized by respiration, presumably by the TCA cycle.

When total seedling lipid was extracted from light- and dark-grown seedlings (Fig. 1, left *y* axis), it was apparent that the lipid content declined from 12 h postimbibition until 3 d postimbibition. From 3 to 5 d postimbibition lipid content was relatively constant, reflecting a constant level of membrane lipids and chlorophyll in young seedlings. Therefore, lipid mobilization appeared to be complete by 3 d postimbibition in *B. napus* cotyledons grown under our laboratory conditions. In contrast, 10 d were required to complete lipid mobilization in castor bean endosperm (Carpenter and Beevers, 1958). Various plants were used in this study. *B. napus* was utilized for in vivo labeling experiments, enzyme assays, immunoblots, and RNA blots. Arabidopsis has a smaller and more completely described genome than *B. napus* and, therefore, was used to clone the genes for NAD$^+$-IDH and fumarase. The enzyme assays, immunoblots, and northern blots of cucumber were necessary to compare our results with the previous data from this plant (Hill et al., 1992).

Activities of NAD$^+$-IDH and Fumarase during Seedling Development in *B. napus* and Cucumber

As shown in Figure 1, gluconeogenesis extended from 12 h to 2 or 3 d postimbibition in developing *B. napus* seedlings. After this period, the in vivo labeling data suggested that the full TCA cycle was operational in these seedlings. The activities of fumarase and NAD$^+$-IDH during this developmental period in *B. napus* and cucumber seedlings are shown in Figure 2. Enzyme activities are reported as total activity per seedling (Fig. 2). Because of the possibility that the efficiency of mitochondrial isolation changed during seedling growth, the data for fumarase and IDH were also reported on the basis of specific activity per milligram of mitochondrial protein (Fig. 2, A and B, insets) for *B. napus*. At all times measured, fumarase total and specific activity were 40- to 100-fold greater than the NAD$^+$-IDH activity in both *B. napus* and cucumber (Fig. 2, note the difference in activity maxima on the *y* axes). Fumarase activity in *B. napus* (Fig. 2A) was low but detectable in seedlings at 12 h postimbibition and then increased rapidly in the light until reaching its maximum total activity at 4 d postimbibition. In the dark-grown seedlings, fumarase followed the same activity profile as in the light but its activity was reduced approximately 3-fold (Fig. 2A). The specific activity of fumarase (Fig. 2A, inset) reached a maximum at d 2 in the light-grown seedlings, 2 d earlier than the maximum total activity. This difference reflects the continuing expansion of the cotyledon concomitantly with general protein synthesis from d 2 to 4 postimbibition. Western analysis (data not presented) showed that fumarase protein level and enzyme activity increased in parallel from 12 h to 5 d postimbibition in the light and in the dark.

A similar activity profile for NAD$^+$-IDH activity in *B. napus* is shown in Figure 2B. These data differ from those for fumarase in two ways. First, the activity of this enzyme was much lower than that of fumarase. Second, and more importantly, NAD$^+$-IDH activity could not be detected by our assay system at 12 h and 1 d postimbibition, either in the dark or in the light. At d 2 through 5, NAD$^+$-IDH activity was present and the light-grown seedling had 3- to 5-fold higher activity than in the dark-grown seedling. Furthermore, extracts from d 1 mitochondria did not alter activity of d 7 mitochondria, showing that soluble factors were not involved. The reduced ratio of released CO_2 to synthesized carbohydrate during the first 2 d postimbibition was due to low or no NAD$^+$-IDH activity as compared with fumarase activity. As with fumarase activity, IDH activity reached a constant specific activity at approximately 2 d postimbibition (Fig. 2B, inset). However, since the seedling was growing, the total activity of IDH per seedling increased linearly (Fig. 2B). Thus, fumarase and NAD$^+$-IDH accumulation appear to be coordinately regulated.

The development of fumarase and NAD$^+$-IDH activities in cucumber seedlings (Fig. 2C) mirrors their activities in *B. napus.* NAD$^+$-IDH activity was undetectable until d 2 postimbibition, whereas fumarase activity could be measured at the first time point, 12 h postimbibition. After d 2, both activities increased with the growth of the seedling. Like *B. napus*, both fumarase and NAD$^+$-IDH activities were reduced in the dark-grown cucumber seedlings, as compared with those grown in the light. Our results differ slightly from previous data with cucumber (Hill et al., 1992). In their study the activity of NAD$^+$-IDH activity in the dark was much lower relative to its activity in the light than what we observed.

Isolation of Arabidopsis NAD$^+$-IDH and Fumarase cDNAs and Immunoblot Analysis of NAD-IDH

To obtain molecular tools for the analysis of fumarase and NAD$^+$-IDH in developing seedlings, these genes were cloned from Arabidopsis (Behal and Oliver, 1997, 1998). *idhI* and *idhII* are 86% identical at the amino acid level and both possess most of the important residues of the catalytic site, as determined from the crystal structure of the

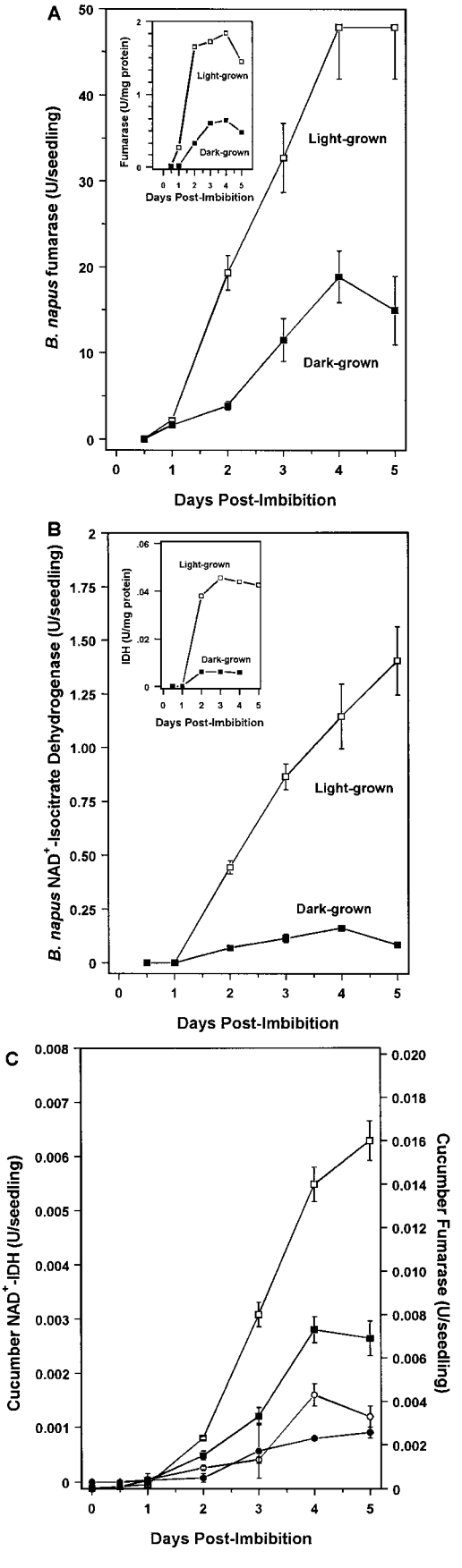

Figure 2. TCA cycle enzyme activities during seedling development. Mitochondrial extracts were prepared as described in "Materials and Methods." Fumarase activity was determined by the malate-dependent increase in A_{240}. NAD^+-IDH activity was determined by monitoring NAD^+ reduction at A_{340} when isocitrate was provided as the substrate. Data represent four replicate experiments for light-grown tissues and two replicate experiments for dark-grown tissues. Both enzymes were assayed in the linear range of their activities. (○) and (●), NAD^+-IDH activity in light- and dark-grown seedlings, respectively; (□) and (■) fumarase activity in light- and dark-grown seedlings, respectively. A, Fumarase activity in developing *B. napus* seedlings expressed as total activity per seedling (U [units]/seedling, main figure) and specific activity (U/mg mitochondrial protein, inset). B, NAD^+-IDH activities in *B. napus* expressed as total activity per seedling and specific activity. C, Fumarase and NAD^+-IDH activities in developing cucumber seedlings expressed as total activity per seedling.

$NADP^+$-IDH protein from *E. coli* (Hurley et al., 1990). The coding region of both of the Arabidopsis *idh* genes is 1100 bp in length and encodes a protein with a predicted molecular mass of 40 kD. When IDH I and IDH II were overexpressed separately in *E. coli*, neither extract displayed NAD^+-dependent IDH activity, although the native $NADP^+$-dependent IDH activity was easily detectable (data not shown). Experiments to denature and refold the recombinant NAD^+-IDH to obtain enzymatic activity were unsuccessful.

The Arabidopsis fumarase gene is 1770 bp in length, encoding a protein with a predicted molecular mass of 52.8 kD, and is highly homologous to the gene isolated from eukaryotes and to the fumarase C gene of bacteria (Behal and Oliver, 1997).

To obtain antibodies for immunoblot analysis of NAD^+-IDH, *idhI and idhII* were overexpressed in *E. coli* without their putative mitochondria-targeting sequences. The Coomassie blue staining of 10 μg of total protein from an extract of induced BL21 (DE3) cells carrying the pET-IDH I plasmid is shown in Figure 3A. The major protein band in this extract migrated at a relative molecular mass of 47 kD (plant NAD^+-IDH migrates at 47 kD despite a molecular mass of 40 kD based on its sequence). Antibody was prepared against this protein and purified on an antigen-linked column. The reaction of this antibody at 1:2000 dilution with 50 ng of total protein from an extract of a pET-IDH I culture is shown in Figure 3B. The purified anti-IDH I antibody detected one band in Arabidopsis (Fig. 3C), cauliflower (Fig. 3D), and pea (Fig. 3E) mitochondria at 47 kD. This antibody recognized multiple bands in *B. napus* at molecular masses greater than 47 kD (Figs. 3F and 4). We observed that, when antioxidant buffer additions were altered, these bands either increased or decreased in intensity. The mitochondrial protocol used, containing the antioxidant and anti-phenolic compounds PVP-40, polyvinylpolypyrrolidone, β-mercaptoethanol, and ascorbate, gave the least amount of cross-reaction with nonspecific bands. *B. napus* seeds have high levels of phenolics in the seed coat and contain 48% lipid. Proteins can be cross-linked by phenolic and lipid-based mechanisms, and lipid peroxidation is a probable mechanism for inactivation of

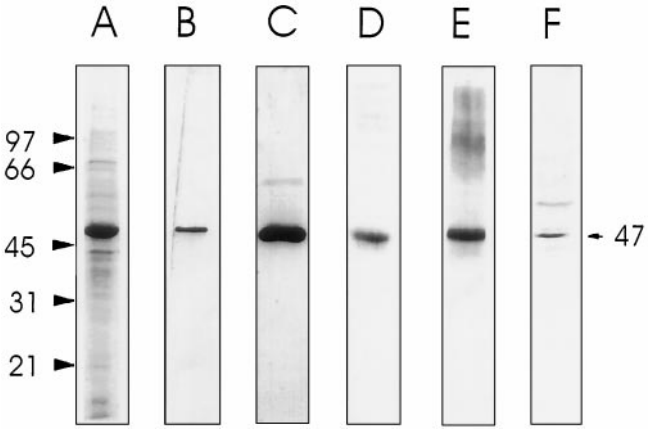

Figure 3. Overexpression of recombinant Arabidopsis IDH I protein in *E. coli* and immunoblot analysis of IDH I in several plants. A to F, Electrophoresis on 12.5% (w/v) acrylamide SDS-PAGE followed by transfer to nitrocellulose in modified Towbin buffer. A, Coomassie blue stain of 10 μg of total protein of recombinant pET-IDHI *E. coli* extract. B, Immunoblot analysis of 50 ng of total protein of recombinant pET-IDHI *E. coli* extract, reacted with anti-IDH at 1:2000 dilution. C to F, Immunoblot analysis of plant mitochondrial extracts with anti-IDH at 1:20 dilution. C, Arabidopsis leaf, 20 μg; D, cauliflower, 20 μg; E, pea leaf, 100 μg; and F, *B. napus* seedling, 3 d postimbibition, 40 μg.

mitochondrial proteins (Cohn et al., 1996). When the antibody was immunoprecipitated against its antigen prior to probing the developmental immunoblot, the 47-kD band representing NAD^+-IDH was preferentially eliminated (Fig. 4C). This further demonstrated that the 47-kD band in the *B. napus* mitochondrial extracts represented NAD^+-IDH. Antibody was also made against IDH II produced using the pMAL overexpression system. This antibody, anti-IDH II, also recognized a protein band at 47 kD in plant mitochondrial extracts.

Occurrence of NAD^+-IDH Protein in Developing Seedlings

As shown in Figure 2, NAD^+-IDH enzyme activity could not be detected until d 2 postimbibition in developing *B. napus* seedlings. To investigate when the NAD^+-IDH protein was synthesized during seedling development, anti-IDH I and anti-IDH II were used to probe the same *B. napus* mitochondrial extracts that had previously been assayed catalytically. Under the conditions of our immunoblot, the NAD^+-IDH I protein was not detectable until 2 d postimbibition in the light (Fig. 4A) or in the dark (Fig. 4B), when equivalent amounts of protein for each time were probed with antibody. Thus, the lack of NAD^+-IDH activity prior to d 2 postimbibition can be explained by the lack of immunodetectable protein.

The anti-IDH I antibody recognized only one of the two potential *idh* gene products of Arabidopsis: it recognized IDH I produced in *E. coli* but not IDH II. It is unknown how many *idh* genes exist in the *B. napus* genome and whether this antibody will recognize all of the gene products. When immunoblot analysis of mitochondrial extracts of developing *B. napus* seedlings was performed with anti-IDH II, no immunoreactive protein of the appropriate size could be detected until the 3rd d postimbibition (data not shown). Since NAD^+-IDH enzyme activity was detected at d 2 postimbibition in these extracts, the discrepancy between the results with these two antibodies could arise from a difference in their sensitivities. Alternatively, IDH I may form a functional homooctamer at d 2 without the contribution of the IDH II protein. The molecular structure of the IDH protein from plants is still uncertain and it is unknown whether both proteins are essential for activity of the holoenzyme (Behal and Oliver, 1998).

Postgerminative Expression of TCA Cycle Genes in *B. napus*

To examine whether the lack of immunodetectable NAD^+-IDH protein until 2 d postimbibition in *B. napus* was due to a lack of its mRNA, RNA-blot analysis was undertaken. Total RNA was isolated from developmentally staged *B. napus* and cucumber seedlings and probed with the full-length *idhI* and *fum* cDNAs. Figure 5 shows the mRNA levels of *idh* and *fum* in *B. napus* and cucumber, from imbibed seeds to seeds at 4 d postimbibition when equivalent amounts of RNA for each time were hybridized with the indicated DNA. As shown in Figure 5A, the *idh* transcript was detectable in seeds and seedlings of *B. napus* allowed to imbibe in the light and in the dark. The level of IDH mRNA was similar for imbibed seeds and at 12 h

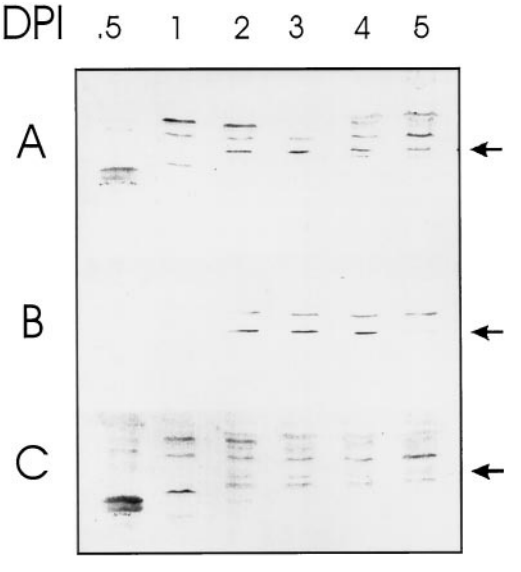

Figure 4. Immunoblot analysis of NAD^+-IDH in *B. napus* mitochondrial extracts during seedling development. A to C, Forty micrograms of total protein from developmentally staged mitochondrial extracts were loaded per lane and electrophoresed on 12.5% (w/v) acrylamide SDS-PAGE. Transfer and immunoblot development were as described in Figure 3 and "Materials and Methods." A, Light-grown tissues. B, Dark-grown tissues. C, Light-grown tissue, probed with anti-IDH I that had been precipitated with recombinant Arabidopsis IDH I prior to incubation with the blot for the purpose of removing IDH-specific antibodies. Arrows indicate IDH band. DPI, Days postimbibition.

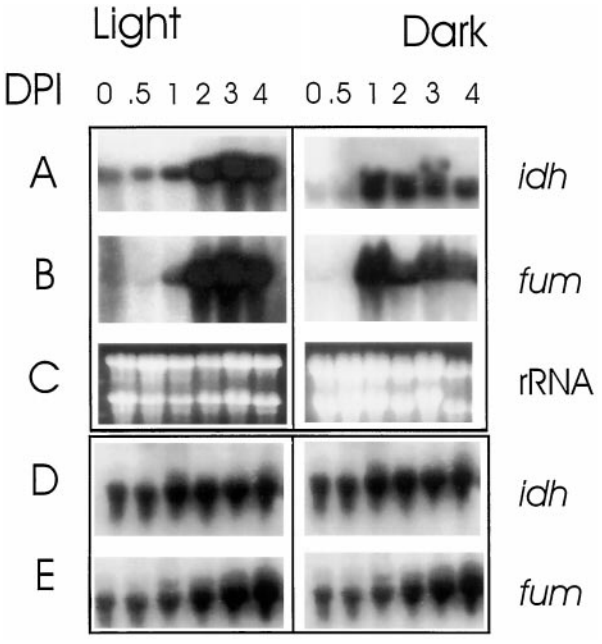

Figure 5. RNA-blot analysis of TCA cycle genes in *B. napus* and cucumber during seedling development in light- and dark-grown tissues. A to E, Ten micrograms of total *B. napus* RNA (A–C) or cucumber RNA (D and E) loaded per lane electrophoresed on a 1.2% (w/v) agarose gel containing 3% (v/v) formaldehyde and blotted onto a nylon membrane. Membranes were hybridized with the ^{32}P-labeled DNA indicated and autoradiographed. A and D, Hybridized with Arabidopsis *idh* cDNA. B and E, Hybridized with Arabidopsis *fum* cDNA. C, Ethidium bromide stain of duplicate gel showing similar loading. DPI, Days postimbibition.

postimbibition. It increased until at least d 3 postimbibition. The transcript level of this gene was reduced in the dark compared with the transcript level in the light in a manner that coincided with the enzyme activity profile for NAD$^+$-IDH. Fumarase mRNA, on the other hand, was not detected until d 1 postimbibition (Fig. 5B). Fumarase enzymatic activity was also detected at this time and it appears that the regulation of this gene occurs primarily at the level of mRNA availability.

RNA-blot analysis in developing cucumber seedlings is shown in Figure 5D (*idh*) and Figure 5E (*fum*). In this plant, *idh* and *fum* mRNA levels are relatively constant throughout development, although there was some increase in the level of both genes at 2 d postimbibition. Since fumarase activity was low and NAD$^+$-IDH activity was not detectable prior to d 2 postimbibition, this blot suggests that in cucumber, both *idh* and *fum* mRNAs experience some posttranscriptional control.

Since the *idh* mRNA was detectable in seeds prior to 2 d postimbibition in *B. napus*, a period when its enzyme activity and protein were not detected, this suggested that there was some posttranscriptional control of *idh* during the gluconeogenic period of *B. napus* seedling development. However, it is possible that, since we probed this RNA blot with the full-length clone, we were detecting the mRNA for only one subunit of a heteromeric protein. Resolution of this question in *B. napus* or cucumber must await cloning of the NAD$^+$-IDH genes from these organisms.

Translational Analysis of *idh* in *B. napus* Seedlings

Since the *idh* mRNA was detectable at 1 d postimbibition in *B. napus* seedlings, whereas both protein and enzyme activity were not detected until d 2, we were interested in determining whether this transcript was actually being translated. We performed a polyribosomal analysis of the *idh* mRNA in 1-d postimbibition seedlings. At d 1 postimbibition, the *B. napus* seed was undergoing gluconeogenesis. At this developmental stage, NAD$^+$-IDH activity and the NAD$^+$-IDH protein were not detected, although the mRNA was present. Two possibilities arise: (a) translational control was preventing the message from being translated, (b) or the message was translated and the protein was rapidly degraded or modified in some way rendering it inactive and undetectable by immunoblot. An RNA-blot analysis of *idh* in the polysomal fractions is shown in Figure 6, and the spectrophotometer trace of the polysome fractionation on a Suc gradient is shown in Figure 6C. This figure demonstrates that the *idh* message was associated with polyribosomes at 1 d postimbibition. This is strong evidence that the NAD$^+$-IDH protein was being made and that regulation of NAD$^+$-IDH during gluconeogenesis was posttranslational.

In light of this finding, we tested two possibilities for the posttranslational modification of NAD$^+$-IDH that could alter both its activity and immunodetectability. Phosphorylation at the active site is a well-documented mechanism of regulating IDH activity in *E. coli* during growth on acetate. Incubation of phosphorylated *E. coli* NADP$^+$-IDH

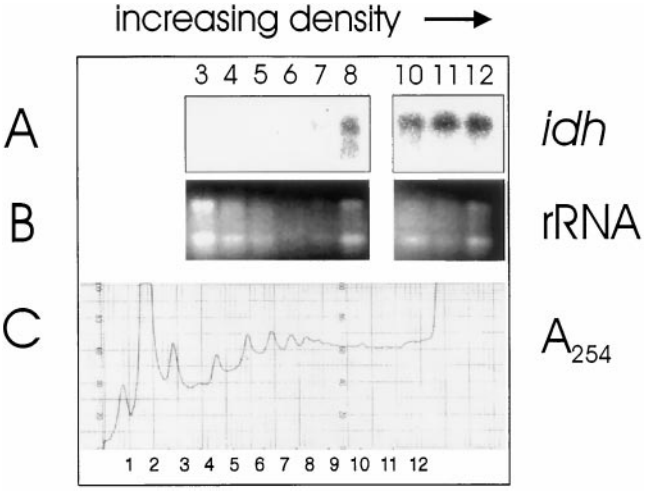

Figure 6. Polysomal RNA-blot analysis of *idh* in 1-d postimbibition *B. napus* seedlings. Polysomes extracted and subjected to Suc-density gradient centrifugation. Resulting gradients were fractionated and A_{254} was monitored. A and B, Ten micrograms of total RNA, obtained after protein extraction by phenol-chloroform, was loaded per lane and electrophoresed on 1.2% (w/v) agarose gel containing 3% formaldehyde. A, Blot probed with Arabidopsis *idh* cDNA. B, Ethidium bromide-stained gel of A. C, Spectrophotometer trace of polysomal fractionation. Lanes in A and B correspond to fractions in C.

with a cellular extract containing IDH phosphatase results in dephosphorylation and renewal of activity (LaPorte et al., 1985). When mitochondrial extracts from 1- and 7-d postimbibition *B. napus* seedlings were incubated with shrimp alkaline phosphatase (1 unit in 1 mL of 20 mM Tris, 10 $MgCl_2$, pH 8.0, for 15 min at room temperature), no change in IDH activity or immunoreactivity was observed (data not shown). Also, as previously mentioned, we determined that there were no soluble inhibitory factors present in d-1 mitochondria that affected activity in d-7 mitochondria.

DISCUSSION

The development of the TCA cycle during oilseed germination and seedling development was examined. In *B. napus* seedlings triacylglycerol metabolism started at imbibition and proceeded until about 3 d postimbibition; after this time the carbon and energy source for seedling growth switched to mainly photosynthetic reactions. Based on the in vivo labeling results, during the period of lipid degradation, metabolism began as gluconeogenic and then switched to being respiratory. This transition was accompanied by a rapid increase in the TCA cycle activities, including fumarase and NAD^+-IDH (Fig. 2). Whereas gluconeogenesis predominated, the decarboxylative reactions of the TCA cycle were bypassed to provide quantitative conversion of lipid to Suc in the cotyledons of the developing seedling. The activity of fumarase, an essential TCA cycle for carbohydrate synthesis from lipid, was detected in *B. napus* seeds 12 h after imbibition. The activity of NAD^+-IDH, a decarboxylative dehydrogenase in the section of the TCA cycle thought to be bypassed during carbohydrate synthesis, was not detected until 2 d postimbibition. Thus, during gluconeogenesis the decarboxylative reactions were bypassed by delaying the expression of NAD^+-IDH (and possibly other enzymes).

Our evidence supports both transcriptional and posttranslational mechanisms of regulation for NAD^+-IDH. The *idh* mRNA was detectable in dry *B. napus* seedlings, and the mRNA level of this gene increased dramatically 2 d postimbibition (Fig. 5). Despite the presence of the message in the dry seed, the protein was not detectable on immunoblots until 2 d postimbibition (Fig. 4) and the enzymatic activity was not detectable either (Fig. 2B). The message was competent for translation, as demonstrated by polysomal analysis (Fig. 6). Thus, at d 1 the NAD^+-IDH message was present and possibly translated, but protein did not accumulate.

After d 2 there was a large increase in both mRNA level and NAD^+-IDH activity, suggesting that at these later times enzyme levels were controlled by mRNA levels. In cucumber it appears that both fumarase and NAD^+-IDH activities were regulated mainly by posttranscriptional events. Whereas the activities of these two enzymes increased steadily during seedling development, the mRNA levels of both genes were relatively constant. Thus, in cucumber, protein expression was controlled at the posttranscriptional level.

Control of the bypass of the TCA cycle by regulation of other respiratory enzymes has been described. Grof et al. (1995) studied the development of the E1α-subunit of pyruvate dehydrogenase during cucumber seedling development. It has been shown that this subunit undergoes light-dependent inactivation by phosphorylation to potentially limit the activity of the TCA cycle during photorespiration (Gemel and Randall, 1992). During germination and early seedling development of cucumber, the steady-state level of the E1α mRNA was maximal 2 d postimbibition. The E1α protein was most active and most abundant at d 4 and 5 postimbibition. The timing of maximal PDC activity corresponded to photosynthetic development. The authors postulated that the delay in PDC activity during seedling development could prevent carbon flow through the full TCA cycle, until the seedling is photosynthetically competent and not dependent on stored cotyledonary reserves.

In conclusion, our data strongly support an interplay of transcriptional and posttranscriptional regulatory mechanisms in the control of NAD^+-IDH during lipid mobilization in developing *B. napus* and cucumber seedlings. Further work will be necessary to address the molecular basis of these control mechanisms.

Received November 10, 1997; accepted March 4, 1998.

LITERATURE CITED

Behal RH, Oliver DJ (1997) Biochemical and molecular characterization of fumarase from plants. Cloning, sequencing, and expression of the *Arabidopsis thaliana* fumarase gene; purification and characterization of *Pisum sativum* fumarase enzyme. Arch Biochem Biophys **347:** 65–74

Behal RH, Oliver DJ (1998) NAD^+-dependent isocitrate dehydrogenase from *Arabidopsis thaliana*. Characterization of two closely related subunits. Plant Mol Biol **36:** 691–698

Canvin DT, Beevers H (1961) Sucrose synthesis from acetate in the germinating castor bean: kinetics and pathway. J Biol Chem **236:** 988–995

Carpenter WD, Beevers H (1958) Distribution and properties of isocitritase in plants. Plant Physiol **34:** 403–409

Cohn JA, Tsai L, Friguet B, Szweda LI (1996) Chemical characterization of a protein-4-hydroxy-2-nonenal cross-link: immunochemical detection in mitochondria exposed to oxidative stress. Arch Biochem Biophys **328:** 158–194

De Vries S, Hoge H, Bisseling T (1988) Isolation of total and polysomal RNA from plant tissues. *In* SB Gelvin, RA Schilperoort, DPS Verma, eds, Plant Molecular Biology Manual, Vol B6. Kluwer Academic Publishers, Dordrecht, The Netherlands, pp 1–13

Gemel J, Randall DD (1992) Light regulation of leaf mitochondrial pyruvate dehydrogenase complex. Role of photorespiratory carbon metabolism. Plant Physiol **100:** 908–814

Grof CPL, Winning BM, Scaysbrook TP, Hill SA, Leaver CJ (1995) Mitochondrial pyruvate dehydrogenase: molecular cloning of the E1α subunit and expression analysis. Plant Physiol **108:** 1623–1629

Hanning I, Heldt HW (1993) On the function of mitochondrial metabolism during photosynthesis in spinach (*Spinacia oleracea* L.) leaves. Partitioning between respiration and export of redox equivalents and precursors for nitrate assimilation products. Plant Physiol **103:** 1147–1154

Hill SA, Bryce JA, Leaver CJ (1994) Pyruvate metabolism in mitochondria from cucumber cotyledons during early seedling development. J Exp Bot **45:** 1489–1491

Hill SA, Groff CPL, Bryce JH, Leaver CJ (1992) Regulation of mitochondrial function and biogenesis in cucumber (*Cucumis sativus* L.) cotyledons during early seedling growth. Plant Physiol **99:** 60–66

Hurley JH, Dean AM, Sohl JL, Koshland DE Jr, Stroud RM (1990) Regulation of an enzyme by phosphorylation at the active site. Science **249:** 1012–1016

Kornberg HL, Krebs HA (1957) Synthesis of cell constituents from C_2-units by a modified tricarboxylic acid cycle. Nature **179:** 988–991

Laemmli UK (1970) Cleavage of structural proteins during the assembly of the head of bacterophage T4. Nature **227:** 680–685

LaPorte DC, Thorsness PE, Koshland DE Jr (1985) Compensatory phosphorylation of isocitrate dehydrogenase: a mechanism for adaptation to the intracellular environment. J Biol Chem **260:** 10563–10568

McIntosh CA, Oliver DJ (1992) NAD^+-linked isocitrate dehydrogenase. Isolation, purification and characterization of the protein from pea mitochondria. Plant Physiol **100:** 69–75

Millhouse J, Wiskich JT, Beevers H (1983) Metabolite oxidation and transport in mitochondria of endosperm from germinating castor bean. Aust J Plant Physiol **10:** 167–177

Oliver DJ, McIntosh CA (1995) The Biochemistry of the Mitochondrial Matrix. *In* CS Levings III, IK Vasil, eds, The Molecular Biology of Plant Mitochondria. Kluwer Academic Publishers, Dordrecht, The Netherlands, pp 237–280

Sambrook J, Fritsch EF, Maniatis T (1989) Molecular Cloning: A Laboratory Manual. Cold Spring Harbor Laboratory Press, Cold Spring Harbor, NY

Schultz DJ, Craig R, Cox-Foster DL, Mumma RO, Medford JI (1994) RNA isolation from recalcitrant tissue. Plant Mol Biol Rep **12:** 310–316

Timberlake WE (1986) Isolation of stage- and cell-specific genes from fungi. *In* J. Bailey, ed, Biology and Molecular Biology of Plant-Pathogen Interactions. North Atlantic Treaty Organization-Advanced Study Institute Series, Vol H1. Springer-Verlag, Berlin, pp 343–357

Towbin H, Staehelin T, Gordon J (1979) Electrophoretic transfer of proteins from polyacrylamide gels to nitrocellulose sheets: procedure and some applications. Proc Natl Acad Sci USA **76:** 4350–4354

Trelease RN, Doman DC (1984) Mobilization of oil and wax reserves. *In* DR Murray, ed, Seed Physiology, Vol 2: Germination and Reserve Mobilization. Academic Press, Orlando, FL, pp 201–245

Voet D, Voet JG (1990) Biochemistry. John Wiley, New York